EUROPEAN ORGANIZATION FOR NUCLEAR RESEARCH

CERN/EP 86-132
12 September 1986

MULTIPLICITY DEPENDENCE OF THE AVERAGE TRANSVERSE MOMENTUM AND OF THE PARTICLE SOURCE SIZE IN p-p INTERACTIONS AT $\sqrt{s}$ = 62, 44 AND 31 GeV

Ames-Bologna-CERN-Dortmund-Heidelberg-Warsaw Collaboration

A. Breakstone[1(*)], R. Campanini[2], H.B. Crawley[1], M. Cuffiani[2], G.M. Dallavalle[3], M.M. Deninno[2], K. Doroba[6], D. Drijard[3], F. Fabbri[2], A. Firestone[1], H.G. Fischer[3], H. Frehse[3(**)], W. Geist[3(***)], H. Flöge[5], L. Gesswein[5], G. Giacomelli[2], R. Gokieli[6], M. Gorbics[1], M. Gorski[3], P. Hanke[5], M. Heiden[3(***)], W. Herr[5(+)], D. Isenhower[1], E.E. Kluge[5], J.W. Lamsa[1], T. Lohse[3], R. Mankel[4], W.T. Meyer[1], T. Nakada[5(++)], M. Panter[3(+++)], A. Putzer[5], K. Rauschnabel[4], B. Rensch[5], F. Rimondi[2], M. Schmelling[4], G.P. Siroli[2(o)], R. Sosnowski[6], M. Szczekowski[6], O. Ullaland[3], D. Wegener[4] and R. Yeung[3(oo)]

1 Ames Laboratory and Physics Department, Iowa State University, Ames, USA
2 Dipartimento di Fisica dell'Università and INFN, Bologna, Italy
3 CERN, European Organization for Nuclear Research, Geneva, Switzerland
4 Institut für Physik der Universität Dortmund, Germany
5 Institut für Hochenergiephysik der Universität Heidelberg, Germany
6 University and Institute for Nuclear Studies, Warsaw, Poland

Submitted to Zeitschrift für Physik C

(*) Present address: University of Hawaii, USA
(**) Present address: CDC, Zürich, Switzerland
(***) Present address: LBL, Berkeley, California, USA
(+) Present address: CERN, Geneva, Switzerland
(++) Present address: SIN, Villigen, Switzerland
(+++) Present address: University of Karlsruhe, Germany
(o) Present address: University of Maryland, USA
(oo) Present address: University of California, Los Angeles, USA

EP/3219P/FF/ef

ABSTRACT

The average transverse momentum and the size of the particle emitting source (measured via Bose-Einstein correlations) have been studied as functions of the charged particle density in the central region in p-p interactions at $\sqrt{s}$ = 62, 44 and 31 GeV. Both the average transverse momentum and the source size increase with increasing density at all three energies. This effect, very weak at $\sqrt{s}$ = 31 GeV, becomes stronger whith increasing energy.

1. INTRODUCTION

Recent experiments at the CERN $\bar{p}p$ collider at various centre of mass energies, $\sqrt{s}$ = 540 GeV [1], $\sqrt{s}$ = 200 and 900 GeV [2] and at the highest ISR energy, $\sqrt{s}$ = 62 GeV [3], have shown that there is an increase in the mean transverse momentum, $\langle p_T \rangle$, with the charged particle density in the central rapidity region, $\rho = \Delta n/\Delta y$. A number of possible explanations for this increase have been proposed. Among these are geometrical models [4], "mini-jets" production [5], and thermodynamical models [6].

An increase of the particle emitting source radius, r, with mean charged multiplicity which may be explained by a geometrical model [7], was measured in a study of Bose-Einstein (B-E) correlations in $\alpha\alpha$ interactions at $\sqrt{s}$ = 126 GeV and in $\bar{p}p$ and pp interactions at $\sqrt{s}$ = 53 and 62 GeV [8]. At $\sqrt{s}$ = 31 GeV [3], no clear evidence of an increasing $\langle p_T \rangle$ with charged multiplicity was observed. Previous measurements of $\langle p_T \rangle$ and r at $\sqrt{s}$ = 19 GeV [9] have also shown no dependence on the charged multiplicity.

It has been suggested recently [10] that in the framework of some thermodynamical models [6,11] one could find a correlation between the dependence on multiplicity of the pions' emitting volume and $\langle p_T \rangle$ which can be used to search for a possible phase transition from hadronic matter to quark-gluon plasma. In such models, the p_T distribution of secondaries reflects both the temperature and the evolution in the transverse direction of the hadronic system, while the central particle density provides a measure of the entropy. The radius, measured via Bose-Einstein correlations, gives information on the final volume of the particle emitting source after a possible expansion following the early stages of the interaction.

In this paper we present the results of a comparative analysis of the dependence of $\langle p_T \rangle$ and r on ρ (the charged particle density in the central region) in pp interactions at $\sqrt{s}$ = 62, 44 and 31 GeV. Previous results on these subjects, with lower statistics, have been presented [3, 12, 13].

2. EXPERIMENT

The experiment was performed at the CERN Intersecting Storage Rings (ISR) using the Split Field Magnet (SFM) detector. The magnetic volume of the detector (with a maximum field strength of 1 Tesla) was filled with Multiwire Proportional Chambers. The momenta of the charged particles were measured over nearly the full solid angle. The performance of the detector is described in previous publications [14].

The experiment used two different triggers: (i) a "minimum bias" trigger, which required the presence of at least one charged track candidate in the detector, accepted about 95% of the inelastic cross section and (ii) an "electron trigger" which selected events with an electron candidate of positive or negative charge produced at a polar angle of 90°. A two-stage Cherenkov counter system was used to identify the electrons. The trigger particles covered a c.m.s. rapidity region $|y| < 0.35$ and an azimuthal angle region $|\phi| < 9°$ [15]. Events were reconstructed with the standard chain of computer programs for the SFM detector. A good vertex fit, defined by a minimum of two charged tracks, was then required for each event. The present analysis is based on ~ 880 000, 460 000 and 1 400 000 "minimum bias" events at $\sqrt{s} = 62$, 44 and 31 GeV respectively and ~ 350 000 "electron trigger" events at $\sqrt{s} = 62$ GeV.

3. ANALYSIS

A number of selection criteria were applied to the data:

(a) The reconstructed interaction vertex was required to be in the overlap region of the two colliding beams.

(b) Low multiplicity events (less than 5 charged particles), which may contain diffraction, were rejected.

(c) In order to remove background from badly measured tracks at large p_T, only particles with $p_T < 3.0$ GeV/c were used.

(d) Tracks were accepted if the estimated relative error in the measurement of their momenta, $\Delta p/p$, was less than 0.8. This cut substantially reduces the number of badly measured tracks and gives $\langle \Delta p/p \rangle \sim 0.18$, independent of multiplicity in the central region.

The charged multiplicity in the central region (defined as $\Delta y = -1.5 < y < 1.5$) was not corrected for acceptance losses. With the above cuts, these losses were estimated to be ~ 20% on average. After the above cuts were applied, we defined the charged particle density, $\rho = \Delta n/\Delta y$, to be the number of charged tracks per unit rapidity interval. All tracks were assumed to be pions.

3.1 Average transverse momentum determination

The average transverse momentum, $\langle p_T \rangle$, was estimated from the arithmetic mean

$$\langle p_T \rangle = \frac{1}{m} \sum_{i=1}^{m} (p_T)_i .$$

Only those tracks in a restricted range, $p_T \in [0.15,\ 2.5]$ GeV/c were used in this calculation in order to avoid acceptance problems at low p_T and to further suppress the contribution from badly measured tracks at large p_T. In terms of the charged particles density, $\rho = \Delta n/\Delta y$, for an event with Δn charged tracks in the rapidity range Δy only the subset of m tracks in the restricted p_T-range was used to estimate the average.

In order to check the validity of the average p_T determination, for some event subsamples a different method was used [12]. Specifically, the p_T distributions of the tracks in the range $0.3 < p_T < 0.8$ GeV/c were fitted to the exponential form $d\sigma/dp_T^2 = A\exp(-bp_T)$. The average transverse momentum was then computed from the fitted value of the slope, i.e. $\langle p_T \rangle = 2/b$. These checks lead to the conclusion that the $\langle p_T \rangle$ dependence on ρ has the same general shape when computed using either of the two methods.

Our reported values of $\langle p_T \rangle$ have not been corrected for acceptance losses. Acceptance corrections have been computed via Monte-Carlo simulation over limited phase-space regions covered by the apparatus. To analyse the effects of the full acceptance, we then proceeded with following two steps:

(a) First we computed the invariant inclusive cross section as a function of p_T and of y in the ranges $0.15 < p_T < 2.5$ GeV/c, $|y| < 1.5$, using only those regions of the apparatus in which the acceptance is well known and above 90%. This yields results in complete agreement with published data at the same energies.

(b) Second, in the same regions used in (a), we computed the acceptance corrected values of p_T distributions. Comparing these corrected values with the uncorrected ones computed on the full apparatus, the differences found in the absolute values of the $\langle p_T \rangle$'s were at most around 20%, but the shape of the $\langle p_T \rangle$ dependence on ρ was essentially unchanged.

This procedure was repeated for different cuts in $\Delta p/p$, azimuthal angle ϕ and Δy, yielding the same conclusions. We present the results from the full apparatus.

3.2 Measurement of the particle source radius

We use Bose-Einstein correlations between like-charged pairs of particles to determine the size of the emitting regions. Results on Bose-Einstein correlations in pp and $\bar{p}p$ interactions at $\sqrt{s} = 62$ GeV and a detailed discussion on the non-interfering background have been published [13]. The following points should be noted:

(a) Since all tracks were assumed to be pions in the analysis, the small contamination by kaons, protons and antiprotons results only in the observed interference effect appearing smaller than reality.

(b) In addition to the cuts mentioned in the previous section, for each particle we required $\Delta p < 0.1$ GeV/c, where Δp is the estimated error in the momentum measurement of the track. This results in a relative error $\langle \Delta p/p \rangle \sim 0.08$ which was observed to be independent of particle density.

(c) As for the average p_T computation, tracks with $p_T < 0.15$ GeV/c were rejected.

(d) Events were kept in the analysis only if they contained at least two positive tracks and one negative track or vice versa in the interval $|y| < 1.5$.

Several parametrizations of the ratio between like and unlike pairs of charged particles, $R = N_L/N_U$, in terms of the variables constructed from the particle momenta were proposed [16]. In this work, R was analysed for different central rapidity densities as a function of the Lorentz invariant quantity for two particles $Q^2(12) = M^2(12) - (m_1 + m_2)^2$ as proposed in ref. [17].

The ratios, R, for different charged particle densities, ρ, were fitted to a function of the form

$$R(Q^2) = \gamma(1 + \alpha e^{-\beta Q^2})(1 + \delta \cdot Q) \; , \tag{1}$$

where the parameter α, which is often called the chaoticity parameter, lies between zero (no Bose-Einstein effects) and one (maximum chaoticity and thus maximum interference). The parameter β is related to the emission radius, ($r = 0.197 \sqrt{\beta}$ fm), γ is a normalization factor and the term $(1 + \delta \cdot Q)$ accounts for the shape of R at large Q, $(Q \equiv \sqrt{Q^2})$. The parametrization (1) gives the space-time dimension of the particle emitting region and leads to values of r somewhat lower than different parametrization used in the literature [18]. All fits had values of χ^2/DOF close to unity.

4. RESULTS

4.1 Average p_T versus ρ for minimum bias data

The average transverse momenta of charged particles, computed in the previously mentioned p_T interval, as functions of the particle density in the central rapidity region, are shown in fig. 1. The plots refer to minimum bias events at $\sqrt{s} = 62$ GeV. In fig. 1(a) the $\langle p_T \rangle$'s for all charged particles are displayed, while figs 1(b) and 1(c) show the same quantities for negative and positive particles separately. The rise of $\langle p_T \rangle$ with the density is clearly seen. Taking the lower boundary of the p_T interval to be $p_T = 300$ MeV/c further enhances the rise of $\langle p_T \rangle$ with ρ, as was shown [3].

The same analysis of $<p_T>$ as a function of ρ has been done for the minimum bias events at $\sqrt{s}$ = 44 and 31 GeV. The results are shown in fig. 2(a) for $\sqrt{s}$ = 44 and in fig. 2(b) for $\sqrt{s}$ = 31 GeV. Comparing with the $\sqrt{s}$ = 62 GeV data one can see that a similar dependence of the $<p_T>$ on ρ is also present at 44 and 31 GeV but the $<p_T>$ rise becomes weaker with decreasing $\sqrt{s}$. The weak rise of $<p_T>$ at 31 GeV was not observed in our previous work [3, 12], in which the statistics were ~ 8 times smaller than available now and the $p_T > 0.15$ GeV/c cut was not applied.

4.2 Average p_T versus ρ for electron trigger data

The mean raw multiplicity in the electron sample, in the central region ($-1.5 < y < 1.5$), is about a factor of 2.5 larger than that of minimum bias events at the same energy. For these data, we analyzed the average p_T dependence on ρ separately for the trigger track and for all the other tracks.

Fig. 3(a) shows the $<p_T>$ of the trigger particle, computed in the p_T range 0.4 - 1.0 GeV/c where the hadronic contamination to the trigger is estimated to be below 30% [15]. Only tracks with $\Delta p/p < 0.30$ have been used. With this cut the $<\Delta p/p>$ of the tracks used in the analysis is 0.09.

The average p_T of all the secondary particles is shown in fig. 3(b). It is computed in the same way as in the minimum bias analysis.

Finally, in fig. 3(c) the average p_T as a function of ρ for non-trigger particles that lie in a ϕ interval of $\pm$ 40° around the trigger track are shown. The $<p_T>$ was computed considering all the tracks (apart from trigger) with $0.15 < p_T < 2.5$ GeV/c.

4.3 Average p_T versus local density

Since it is known [19] that the particle density reaches its highest values when $|y| \rightarrow 0$, we recompute the average p_T and all particle densities taking into account only those tracks in the rapidity interval $-0.5 < y < 0.5$. The results for the minimum bias data at $\sqrt{s}$ = 62 GeV are shown in fig. 4(a). In fig. 4(b), we show the $<p_T>$ of the trigger track in the electron trigger sample ($0.4 < p_T < 1.0$ GeV/c) as a function of ρ, where in this case ρ is computed taking only those tracks lying in an interval $\Delta y = 1$ centred around the trigger particle rapidity.

4.4 Source dimensions

Figs 5(a), 5(c) and 5(d) show the radius r of the particle emitting region as a function of ρ at $\sqrt{s} = 62$, 44 and 31 GeV, respectively. A clear rise of r with increasing particle density is visible in the data at $\sqrt{s} = 62$ GeV, ranging from ~ 0.72 fm for $\rho < 2$ up to ~ 1.7 fm at $\rho \sim 6$. It was pointed out [18] that, due to the finite momentum resolution, the maximum measured value of r can only be an underestimate of the true maximum value. A very weak dependence of r on the particle density in the central region is observed at $\sqrt{s} = 31$ GeV (fig. 5(d)), while a rise of r with ρ is observed at 44 GeV in the ρ region between 1 and 4. The values of r as a function of ρ for electron trigger events are presented in fig. 5(b). They range from ~ 0.8 at ρ around 2 to about 1.3 at ρ around 6.

The values of the chaoticity parameter α, as shown in figs 6(a)-6(d), lie between 0.50 and 0.30, and decrease slowly with increasing multiplicity, at least up to ρ around 4, for all the three energies. The behaviour shown in figs 6(a)-6(c) is in agreement with previous results at ISR energies [8].

5. CONCLUSIONS

We have performed an analysis of the behaviour of the average transverse momentum and of the size of the particle emitting region as a function of the charged particle density variable, $\rho = \Delta n/\Delta y$, at $\sqrt{s} = 62$, 44 and 31 GeV using minimum bias trigger events. An additional sample of electron trigger events at $\sqrt{s} = 62$ GeV was also analyzed. The main results are:

(i) The mean transverse momentum increases with increasing ρ at all energies. The rise of $<p_T>$ becomes steeper when $\sqrt{s}$ increases from 31 to 62 GeV. In the electron trigger events an increase of the $<p_T>$ of the trigger particle, as well as of the non-trigger particles, with increasing ρ is observed. Qualitatively the rise is approximatively linear in all cases, up to ρ around 4-5. In this region a flat distribution is visible which, when going to local density, is moved to values of ρ around 6-7.

(ii) Also the particle source size increases with particle density. The rise, very weak at 31 GeV, becomes clear at $\sqrt{s}$ = 62 GeV both in the minimum bias data and in the electron trigger data. The chaoticity parameter α slowly decreases with ρ at all energies at least for $\rho < 4$.

Acknowledgements

This experiment was greatly helped by contributions from the SFM Detector Group. We are indebted to the ISR Experimental Support Group. We would also like to thank N. Rivoire for her important help. The Dortmund and Heidelberg Groups were supported by a grant from Bundesministerium für Forschung und Technologie of the Federal Republic of Germany. The Ames Group was supported by the United States Department of Energy.

REFERENCES

[1] G. Arnison et al., Phys. Lett. 118B (1982) 167;

G. Ciapetti, Proceedings of the Vth Topical Workshop on Proton Antiproton Collider Physics, St. Vincent (1985).

[2] F. Ceradini, Proceedings of the International Conference on High-Energy Physics, Bari (1985).

[3] A. Breakstone et al., Phys. Lett. 132B (1983) 463.

[4] S. Barshay, Phys. Lett. 127B (1983) 129.

[5] M. Jacob, preprint CERN/TH 3515 (1983).

[6] L. Van Hove, Phys. Lett. 118B (1982) 138.

[7] S. Barshay, Phys. Lett. 130B (1983) 220.

[8] T. Åkesson et al., Phys. Lett. 129B (1983) 269;

T. Åkesson et al., Phys. Lett. 155B (1985) 128.

[9] C. De Marzo et al., Phys. Rev. 29D (1984) 363.

[10] R. Campanini, Lett. al Nuovo Cimento 44 (1985) 343;

R. Campanini, Possible evidence of phase transition to quark gluon plasma at CERN ISR and SPS Collider, preprint DFUB 17/85 (1985).

[11] E.V. Shuryak, Phys. Rep. 61 (1980) 71.

[12] A. Breakstone et al., Multiplicity dependence of transverse momentum spectra at ISR energies, EPS, Bari (1985).

[13] A. Breakstone et al., Phys. Lett. 162B (1985) 400.

[14] M. Della Negra et al., Nucl. Phys. B127 (1977) 1;

W. Bell et al., Nucl. Instr. and Meth. 156 (1978) 111.

[15] D. Drijard et al., Phys. Lett. 108B (1982) 361;

M. Heiden, Ph.D. Thesis, Heidelberg (1981).

[16] G.Goldhaber, The GGLP effect from 1959 to 1985, report LBL-19417 (1985).

[17] G. Goldhaber, Multipion Correlations in e^+e^- Annihilation at SPEAR, presented at the International Conference on High Energy Physics, Lisbon 1981 and LBL-13291 report.

[18] H. Aihara et al, Phys. Rev. D31 (1985) 996.

[19] W. Thomé et al., Nucl. Phys. B129 (1977) 365;

W. Bell et al., Zeitschr. für Phys. C27 (1985) 191.

FIGURE CAPTIONS

Fig. 1 (a) The average transverse momentum of charged particles, with $0.15 \leq p_T \leq 2.5$ GeV/c, produced in the central region of rapidity (|y| 1.5) plotted versus charged particle density ρ, at $\sqrt{s} = 62$ GeV.

(b) Same as in (a) for negative particles only.

(c) Same as in (a) for positive particles only.

Fig. 2 The average transverse momentum of charged particles, with $0.15 \leq p_T \leq 2.5$ GeV/c, produced in the central region of rapidity ($|y| < 1.5$), plotted versus charged particle density, at (a) $\sqrt{s} = 44$ GeV and (b) $\sqrt{s} = 31$ GeV.

Fig. 3 Electron trigger data; $\sqrt{s} = 62$ GeV:

(a) The average transverse momentum of the triggering particle with $0.4 < p_T < 1$ GeV/c, as a function of $\rho = \Delta n/\Delta y$.

(b) The average transverse momentum of all the non-trigger particles having $0.15 \leq p_T \leq 2.5$ GeV/c as a function of ρ.

(c) The average transverse momentum for non-trigger particles, with $0.15 \leq p_T \leq 2.5$ GeV/c, lying in a ϕ interval of $\pm 40°$ around the trigger track.

Fig. 4 (a) The average transverse momentum for tracks having $0.15 \leq p_T \leq 2.5$ GeV/c and $|y| < 0.5$ as a function of the particle density in the same y interval for minimum bias data at $\sqrt{s} = 63$ GeV.

(b) Electron trigger data. The average transverse momentum of the triggering track as a function of the particle density computed for the y interval ± 0.5 around the triggering track rapidity.

Fig. 5 Radius of the particle emitting source as a function of ρ:

(a) Minimum bias trigger at $\sqrt{s} = 62$ GeV.
(b) Electron trigger at $\sqrt{s} = 62$ GeV.
(c) Minimum bias trigger at $\sqrt{s} = 44$ GeV.
(d) Minimum bias trigger at $\sqrt{s} = 31$ GeV.

FIGURE CAPTIONS (Cont'd)

Fig. 6 Chaoticity parameter α as a function of ρ:

(a) Minimum bias trigger at $\sqrt{s}$ = 62 GeV.
(b) Electron trigger at $\sqrt{s}$ = 62 GeV.
(c) Minimum bias trigger at $\sqrt{s}$ = 44 GeV.
(d) Minimum bias trigger at $\sqrt{s}$ = 31 GeV.

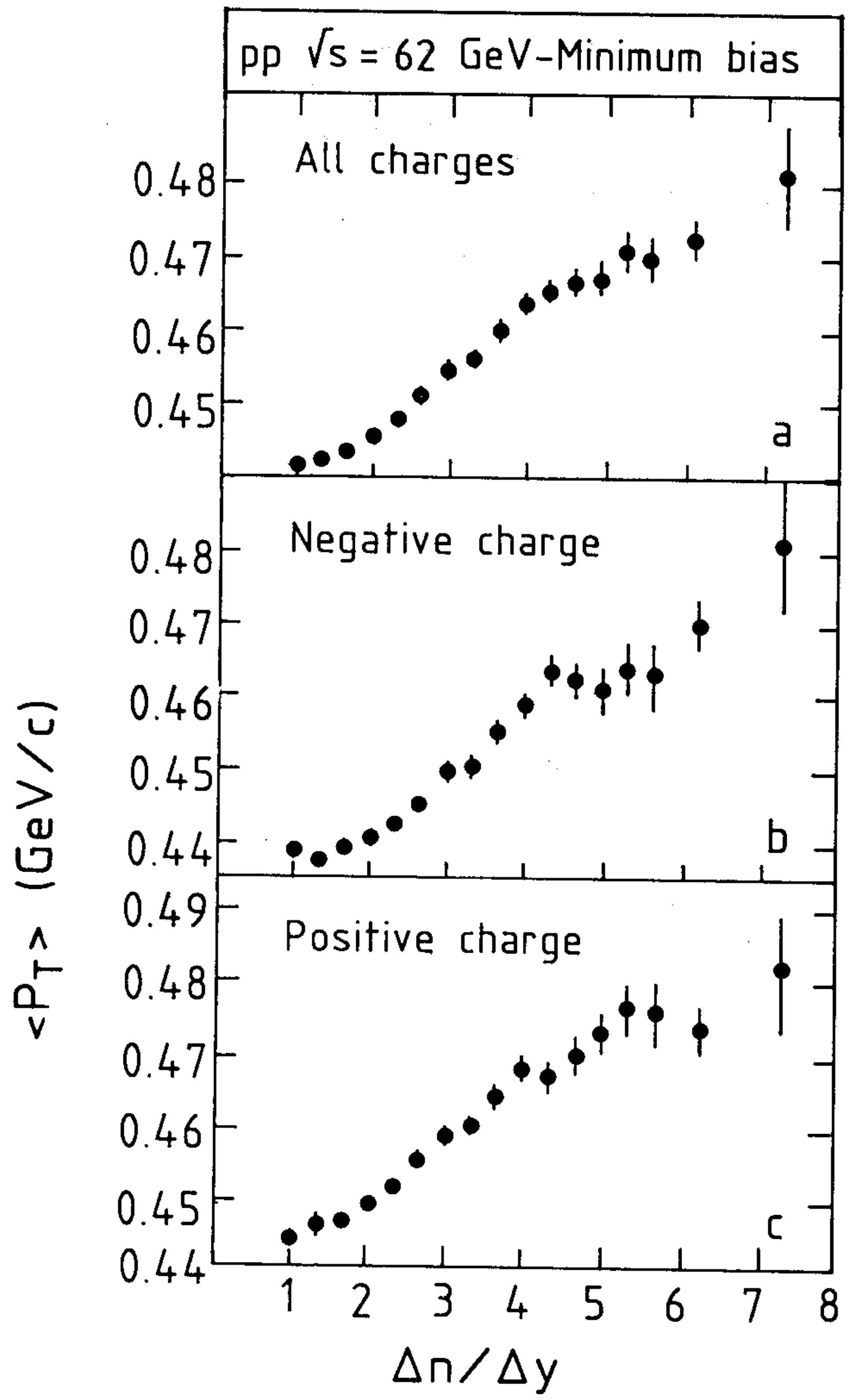
pp √s = 62 GeV-Minimum bias
All charges
a
Negative charge
b
Positive charge
c
0.44
0.45
0.46
0.47
0.48
0.49
<P_T> (GeV/c)
1
2
3
4
5
6
7
8
Δn/Δy

Fig. 1

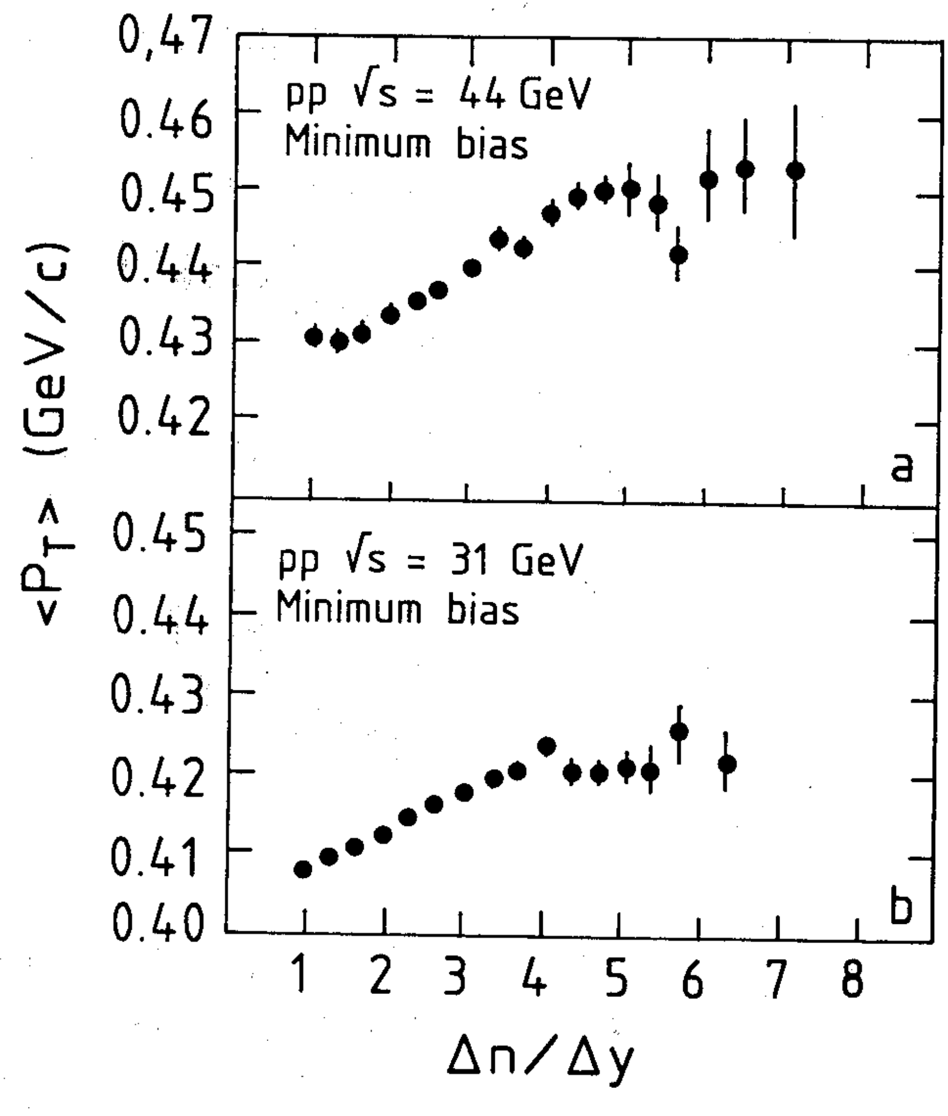

0,47
0.46
0.45
0.44
0.43
0.42
pp √s = 44 GeV
Minimum bias
a
0.45
0.44
0.43
0.42
0.41
0.40
pp √s = 31 GeV
Minimum bias
b
1 2 3 4 5 6 7 8
<P_T> (GeV/c)
Δn/Δy

Fig. 2

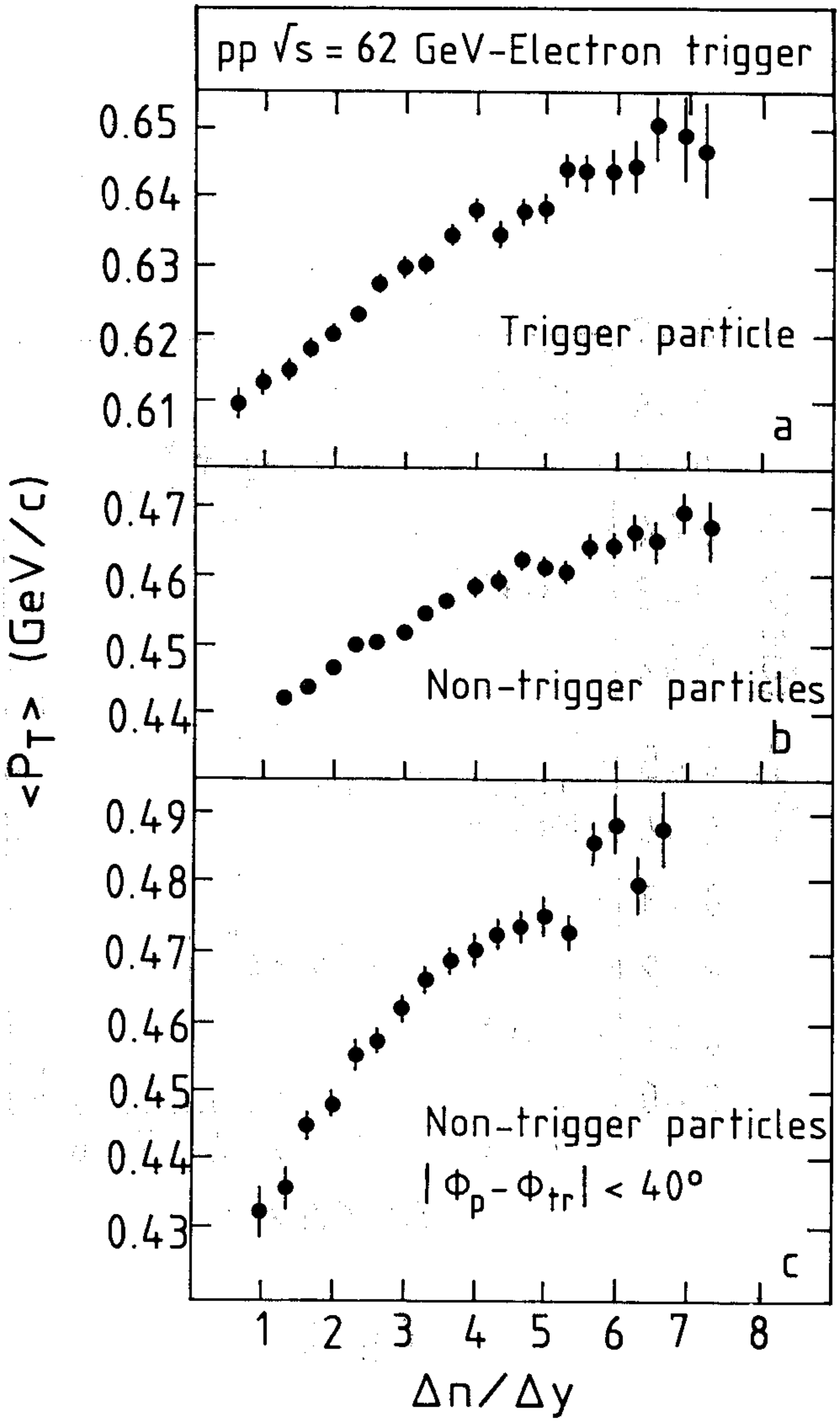
pp √s = 62 GeV-Electron trigger
0.65
0.64
0.63
0.62
0.61
Trigger particle
a
0.47
0.46
0.45
0.44
Non-trigger particles
b
0.49
0.48
0.47
0.46
0.45
0.44
0.43
Non-trigger particles
|Φp - Φtr| < 40°
c
<PT> (GeV/c)
1
2
3
4
5
6
7
8
Δn/Δy

Fig. 3

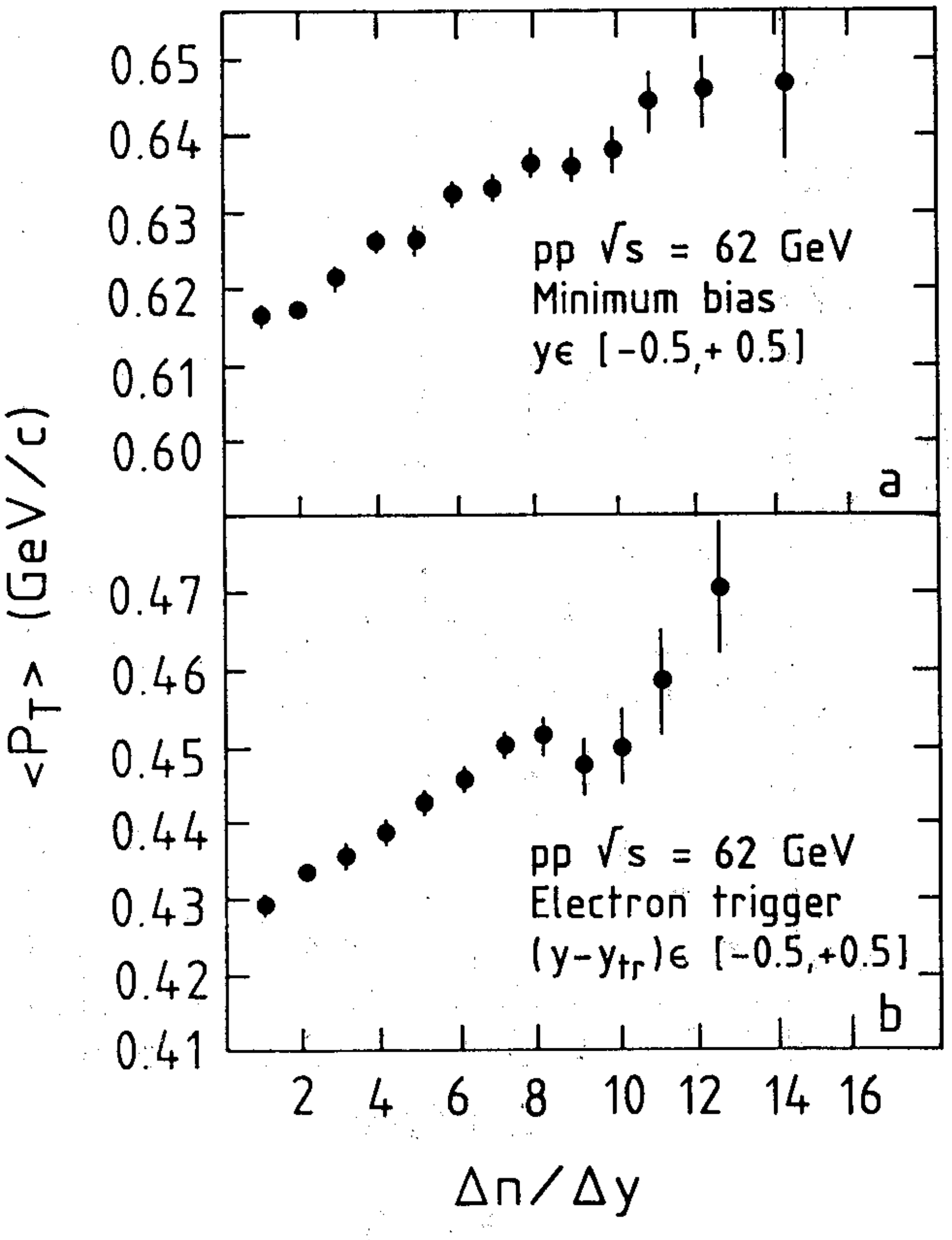
0.65
0.64
0.63
0.62
0.61
0.60
pp √s = 62 GeV
Minimum bias
y∈ [-0.5,+ 0.5]
a
0.47
0.46
0.45
0.44
0.43
0.42
0.41
pp √s = 62 GeV
Electron trigger
(y-y_tr)∈ [-0.5,+0.5]
b
<P_T> (GeV/c)
2
4
6
8
10
12
14
16
Δn/Δy

Fig. 4

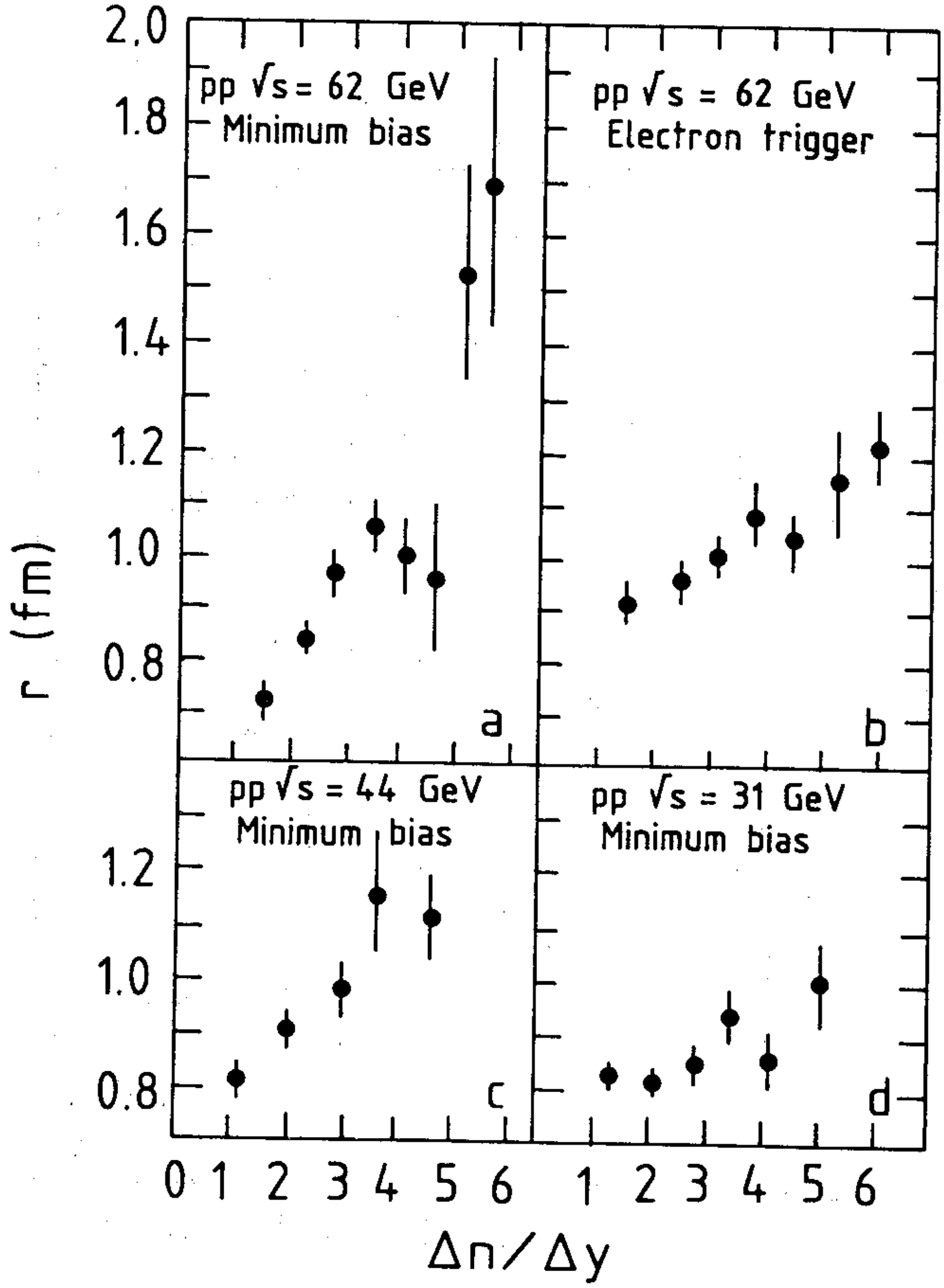

pp √s = 62 GeV
Minimum bias
pp √s = 62 GeV
Electron trigger
pp √s = 44 GeV
Minimum bias
pp √s = 31 GeV
Minimum bias
a
b
c
d
r (fm)
Δn/Δy
2.0
1.8
1.6
1.4
1.2
1.0
0.8
0 1 2 3 4 5 6

Fig. 5

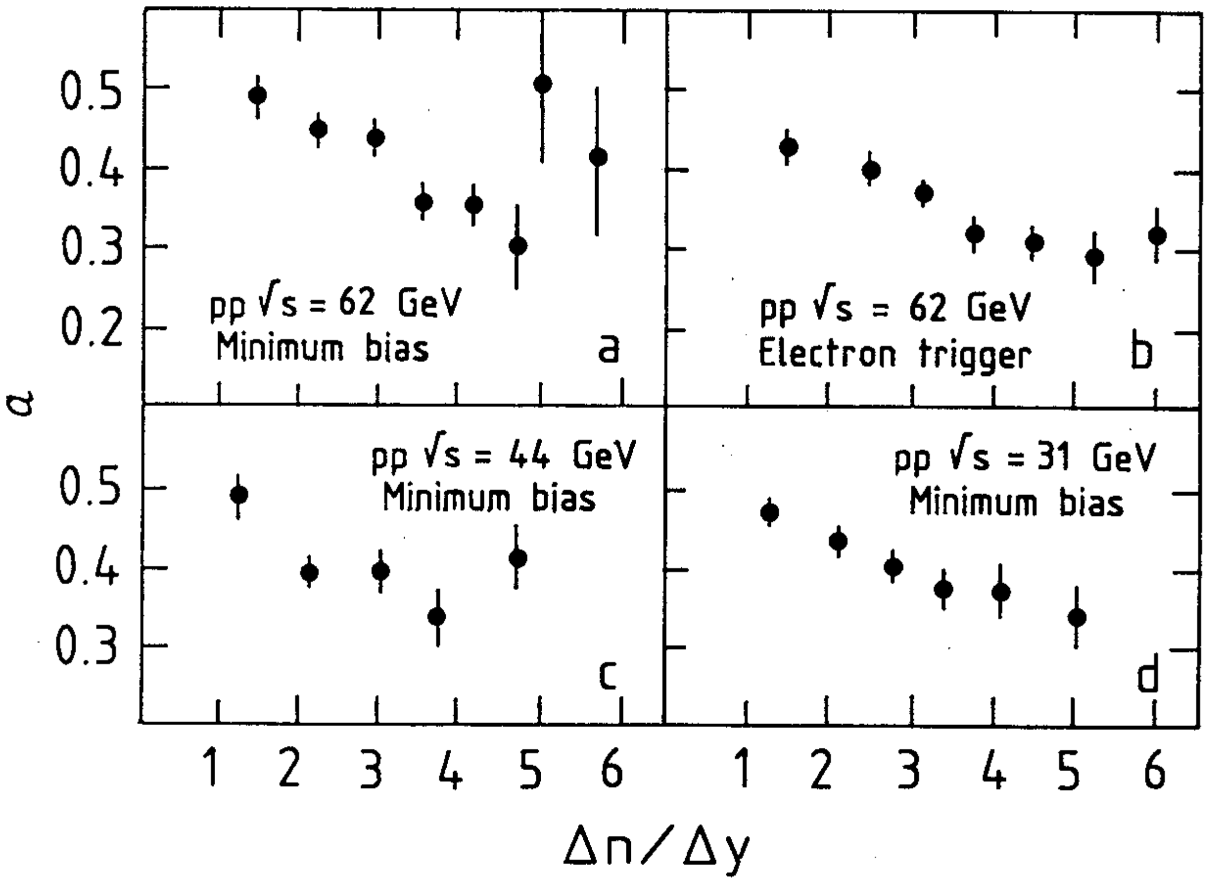
0.5
0.4
0.3
0.2
a
pp √s = 62 GeV
Minimum bias
a
pp √s = 62 GeV
Electron trigger
b
pp √s = 44 GeV
Minimum bias
c
pp √s = 31 GeV
Minimum bias
d
1 2 3 4 5 6
Δn/Δy

Fig. 6